Defective Oxidative Phosphorylation in Thyroid Oncocytic Carcinoma Is Associated with Pathogenic Mitochondrial DNA Mutations Affecting Complexes I and III

Elena Bonora,[1] Anna Maria Porcelli,[2] Giuseppe Gasparre,[1] Annalisa Biondi,[3] Anna Ghelli,[2] Valerio Carelli,[4] Alessandra Baracca,[3] Giovanni Tallini,[5] Andrea Martinuzzi,[6] Giorgio Lenaz,[3] Michela Rugolo,[2] and Giovanni Romeo[1]

[1]Unità di Genetica Medica, Policlinico Universitario S. Orsola-Malpighi; [2]Dipartimento di Biologia Evoluzionistica Sperimentale, [3]Dipartimento di Biochimica, [4]Dipartimento di Scienze Neurologiche, and [5]Dipartimento di Anatomia Patologica, Università di Bologna, Bologna, Italy; and [6]Istituto Scientifico "E. Medea," Conegliano Veneto, Italy

Abstract

Oncocytic tumors are characterized by cells with an aberrant accumulation of mitochondria. To assess mitochondrial function in neoplastic oncocytic cells, we studied the thyroid oncocytic cell line XTC.UC1 and compared it with other thyroid non-oncocytic cell lines. Only XTC.UC1 cells were unable to survive in galactose, a condition forcing cells to rely solely on mitochondria for energy production. The rate of respiration and mitochondrial ATP synthesis driven by complex I substrates was severely reduced in XTC.UC1 cells. Furthermore, the enzymatic activity of complexes I and III was dramatically decreased in these cells compared with controls, in conjunction with a strongly enhanced production of reactive oxygen species. Osteosarcoma-derived transmitochondrial cell hybrids (cybrids) carrying XTC.UC1 mitochondrial DNA (mtDNA) were generated to discriminate whether the energetic failure depended on mitochondrial or nuclear DNA mutations. In galactose medium, XTC.UC1 cybrid clones showed reduced viability and ATP content, similarly to the parental XTC.UC1, clearly pointing to the existence of mtDNA alterations. Sequencing of XTC.UC1 mtDNA identified a frameshift mutation in ND1 and a nonconservative substitution in cytochrome *b*, two mutations with a clear pathogenic potential. In conclusion, this is the first demonstration that mitochondrial dysfunction of XTC.UC1 is due to a combined complex I/III defect associated with mtDNA mutations, as proven by the transfer of the defective energetic phenotype with the mitochondrial genome into the cybrids. (Cancer Res 2006; 66(12): 6087-96)

Introduction

Oncocytic adenomas and carcinomas are a subset of thyroid tumors predominantly composed (at least 75%) of oncocytic cells. These cells are characterized by an aberrant accumulation of mitochondria that results in a distinctive granular eosinophilic appearance in conventional histology sections. Tumors composed of oncocytic cells may occur at a variety of sites but are particularly common among thyroid tumors of follicular cell derivation (1). Oncocytic thyroid tumors have long been suspected to be more aggressive than their non-oncocytic counterparts (1) and the presence of oncocytic features is now considered an adverse prognostic indicator for follicular thyroid carcinomas (2). Decreased survival in patients with oncocytic carcinomas may be due to reduced competence in iodine uptake by the tumor cells, resulting in poor response to radioiodine treatment (1). Thyroid oncocytic cells have been associated with mitochondrial abnormalities, such as loss of electron transport components, deficiencies in energy-related functions, and impaired protein synthesis (3). The mitochondrial respiratory chain is a major source of reactive oxygen species (ROS), which in excess can damage mitochondria and mitochondrial DNA (mtDNA), eventually contributing to the promotion of tumor development. Mitochondrial abnormalities have in fact been described in many tumors (4, 5). The main sources of mitochondrial ROS are complex I and complex III of the respiratory chain (6). It is worth noting that many mtDNA nucleotide changes have been found in complex I and IV subunit genes in thyroid tumors (3, 7, 8). However, the functional relevance of these mutations on the biochemical phenotype has not been investigated.

Defective mitochondrial ATP synthesis has been reported in thyroid oncocytomas, suggesting that an impaired oxidative phosphorylation might induce mitochondrial hyperplasia and proliferation in these tumors as a compensatory mechanism (9, 10).

To assess the bioenergetic efficiency of mitochondria, we analyzed the thyroid oncocytic follicular cell line XTC.UC1 and compared it with other non-oncocytic lines of follicular cell derivation. In this study, we show that only XTC.UC1 cells exhibited a remarkable loss of viability when glycolysis is dramatically reduced and cells are forced to rely solely on mitochondria for ATP production (11). Furthermore, the rate of ATP synthesis and oxygen consumption driven by complex I substrates and the complex I/III enzymatic activities were all significantly decreased. This biochemical phenotype was cotransferred into the transmitochondrial cell hybrid (cybrid) model with the XTC.UC1 mtDNA, indicating that mutations in this genome are responsible for the respiratory defect. Entire mtDNA sequencing indeed revealed two mutations in complex I and complex III subunit genes, which fulfill the main criteria for being pathogenic. These combined functional and molecular approaches have allowed us to correlate for the first time the bioenergetic defect with the presence of mtDNA mutations in an oncocytic cell model.

Note: A.M. Porcelli, G. Gasparre, and A. Biondi are co-first authors.

Requests for reprints: Elena Bonora, Unità di Genetica Medica, Dip. Medicina Interna, Policlinico Universitario S. Orsola-Malpighi, Via Massarenti 9, 40138 Bologna, Italy. Phone: 39-051-429-2007; Fax: 39-051-636-4004; E-mail: elena.bonora@eurogene.org.

doi:10.1158/0008-5472.CAN-06-0171

Materials and Methods

Materials. Carbonyl cyanide *p*-(trifluoro-methoxy)phenylhydrazone, 3-(4,5-dimethylthiazol-2-yl)-2,5-diphenyltetrazolium bromide (MTT), rotenone, antimycin A, ADP, and ATP were purchased from Sigma (Milan, Italy). Dichlorodihydrofluorescein diacetate was from Molecular Probes (Invitrogen, Milan, Italy). ATP monitoring kit was from BioOrbit (Turku, Finland). Antibodies used for Western blot were mouse antibodies for complex I, II, and IV subunits, purchased in cocktails from MitoSciences (Eugene, OR); rabbit polyclonal antibody against human ND1 subunit, a kind gift from Dr. A. Lombes (Institut National de la Sante et de la Recherche Medicale, Hospital Salpetriere, Paris, France); rabbit antibody for complex III, a kind gift from Prof. C. Godinot (University Claude Bernard de Lyon, France); and mouse monoclonal antibody for porin, purchased from Molecular Probes (Invitrogen).

Cell cultures and growth conditions. Human thyroid carcinoma cell lines used are oncocytic carcinoma cell line XTC.UC1 (derived from metastasis in the mammary gland of an oncocytic thyroid tumor; ref. 12) and non-oncocytic cell lines TPC-1 (derived from human papillary thyroid tumor), WRO (derived from human follicular thyroid tumor), and TAD-2 (human fetal thyroid cells). XTC.UC1 cells were grown in DMEM whereas the others in RPMI medium. Both media contained 10% fetal bovine serum (FBS), 2 mmol/L L-glutamine, 100 units/mL penicillin, and 100 μg/mL streptomycin.

Cybrid clones (HXTC) were constructed using enucleated XTC1.UC1 cells as mitochondria donors and the osteosarcoma 143B.TK$^-$-derived Rho-0 cells as acceptors [kindly provided by Giuseppe Attardi (Division of Biology, California Institute of Technology, Pasadena, CA) and Michael King (Department of Biochemistry and Molecular Pharmacology, Thomas Jefferson University, Philadelphia, PA)]. The cybrid control cell line was the same as described in ref. 13. Cybrid cell lines were grown in DMEM with 10% FBS, 2 mmol/L L-glutamine, 100 units/mL penicillin, 100 μg/mL streptomycin, 0.1 mg/mL bromodeoxyuridine, and 50 μg/mL uridine. Cultures were grown in a humidified incubator at 37°C with 5% CO_2.

Cell viability measurement. Cells (4×10^4) were seeded into 24-well plates and, after 24 hours, were incubated in DMEM glucose-free medium supplemented with 5 mmol/L galactose, 5 mmol/L Na-pyruvate, and 10% FBS (DMEM-galactose medium). The MTT assay was done as previously described (14).

ATP assay. The amount of cellular ATP was determined by using the luciferin/luciferase assay as previously described (13). The measurements of mitochondrial ATP synthesis were done in cells grown in DMEM-glucose according to ref. 15 with minor modifications. Briefly, after trypsinization, cells were resuspended (7×10^6/mL) in buffer A [10 mmol/L KCl,

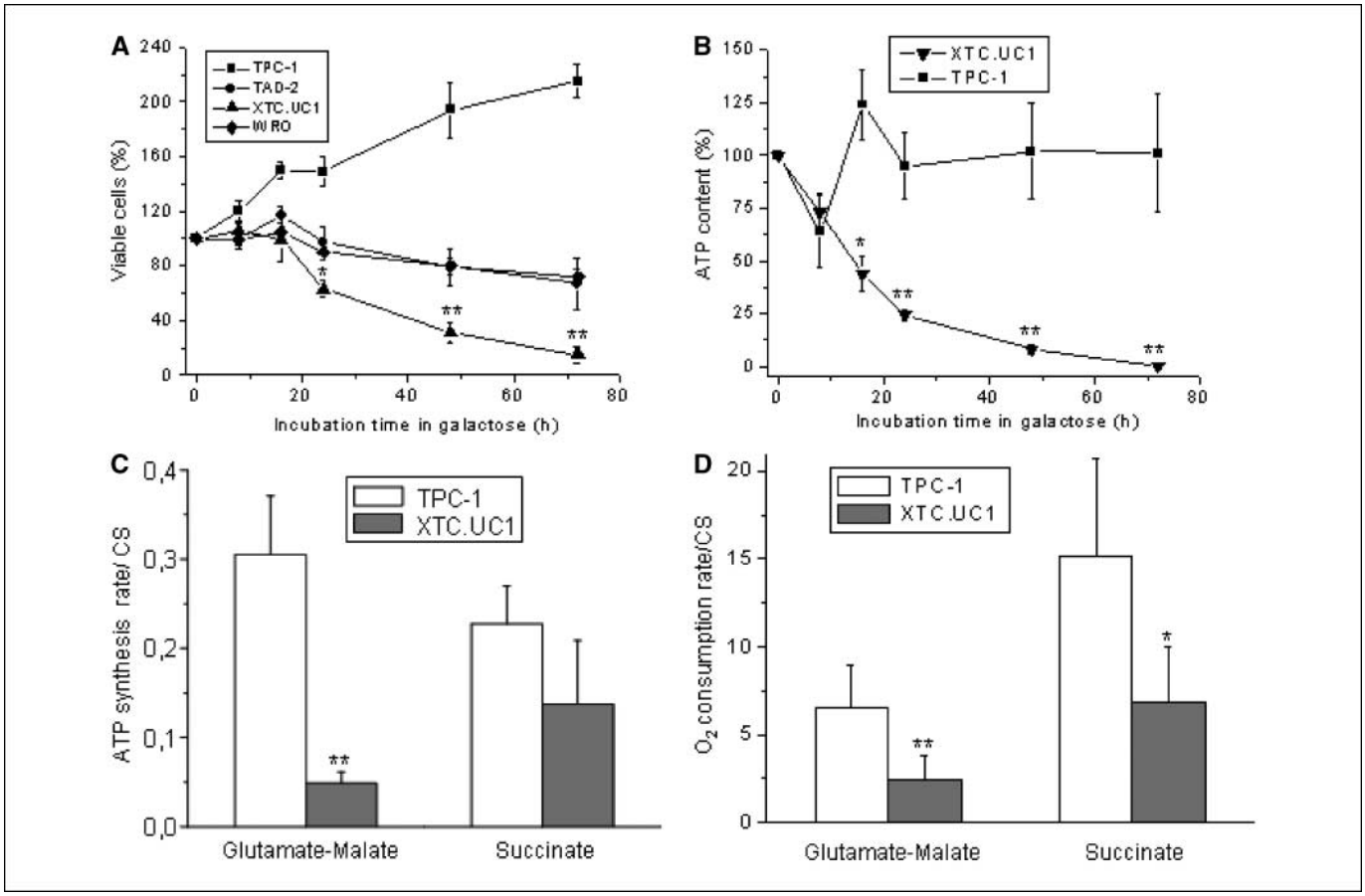

Figure 1. Determination of cell viability and oxidative phosphorylation efficiency in different thyroid cell lines. Cell lines were incubated in DMEM-galactose medium for the times indicated. *A,* cell viability was determined using the MTT assay. MTT absorbance value at time 0 was considered as the 100% value of viable cells. *Points,* mean of three to five experiments; *bars,* SD. *, $P < 0.05$; **, $P < 0.01$, values significantly different from that of the other cell lines. *B,* ATP content was determined as described in Materials and Methods. Data are expressed as percent of ATP levels determined in DMEM-glucose (time 0). *Points,* mean of three to five experiments; *bars,* SD. *, $P < 0.05$; **, $P < 0.01$, values significantly different from that of TPC-1 cells. *C,* the rate of mitochondrial ATP synthesis was determined in cells treated with 50 μg/mL digitonin. ATP synthesis driven by complex I (glutamate plus malate) or complex II (succinate plus rotenone) substrates was determined as described in Materials and Methods. The rates of ATP synthesis (nmol/min/mg) were normalized for citrate synthase (*CS*) activity of the corresponding sample. *Columns,* mean (TPC-1, $n = 6$; XTC.UC1, $n = 9$); *bars,* SD. **, $P < 0.01$, values significantly different from that of TPC-1 cells. *D,* respiration measurements were done in digitonin-permeabilized cells, as described in Materials and Methods, in the presence of ADP (state 3). Respiratory rates (nmol O_2/min/mg protein) are reported after normalization of the polarographic oxygen consumption rates to citrate synthase activity. *Columns,* mean; *bars,* SD. *, $P < 0.05$; **, $P < 0.01$, values significantly different from that of TPC-1.

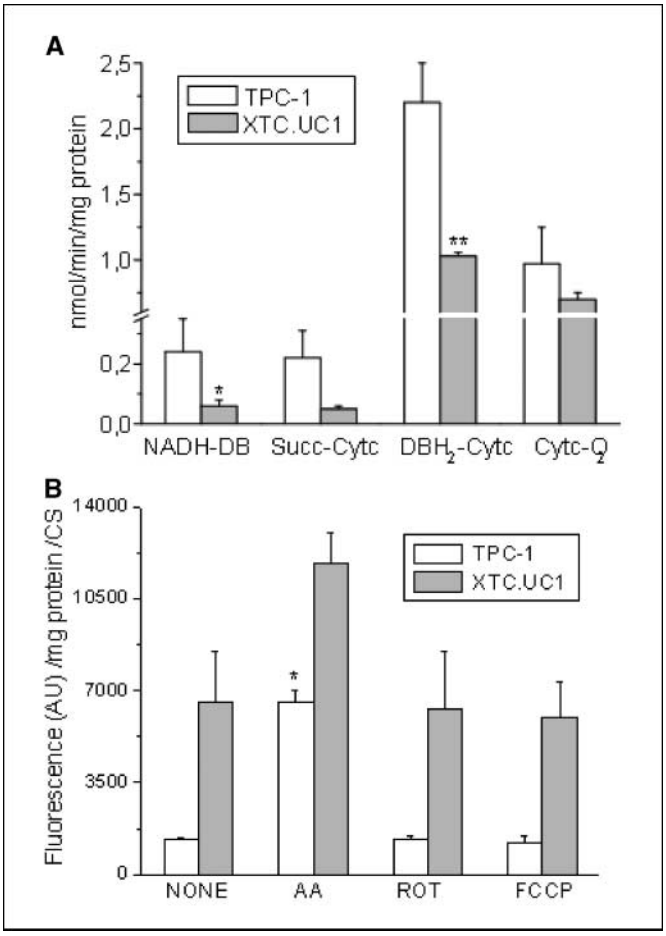

Figure 2. Respiratory chain oxidoreductase activities and ROS production. *A,* complex I, complex II + complex III, complex III, and complex IV activities were determined in isolated mitochondria of both TPC-1 and XTC.UC1 cell lines as described in Materials and Methods. *Columns,* mean; *bars,* SD. *, $P < 0.05$; **, $P < 0.01$, values significantly different from that of TPC-1 cells. *B,* ROS production was determined by dichlorodihydrofluorescein diacetate fluorescence in the presence of the indicated inhibitors of respiration and of carbonyl cyanide *p*-(trifluoro-methoxy)phenylhydrazone (*FCCP*). Data were expressed as fluorescence (arbitrary units) per milligram of protein and normalized to citrate synthase activity. *Columns,* mean; *bars,* SD. *, $P < 0.01$; the fluorescence of untreated cells (*NONE*) is used as a reference for statistical significance. All fluorescence values of XTC.UC1 cells were significantly different from that of TPC-1 cells ($P < 0.002$ for rotenone; $P < 0.001$ for all others).

25 mmol/L Tris-HCl, 2 mmol/L EDTA, 0.1% bovine serum albumin, 10 mmol/L potassium phosphate, 0.1 mmol/L $MgCl_2$ (pH 7.4)], kept for 15 minutes at room temperature, and then incubated with 50 μg/mL digitonin for 1 minute. After centrifugation, the cell pellet was resuspended in buffer A and aliquots were taken to measure ATP synthesis, protein content (16), and citrate synthase activity (17). Aliquots of cells were incubated with 5 mmol/L malate plus 5 mmol/L glutamate (complex I–driven substrates) in the presence or absence of 10 μg/mL oligomycin, or with 10 mmol/L succinate plus 2 μg/mL rotenone (complex II–driven substrate), and 0.2 mmol/L ADP for 1 and 3 minutes. The amount of ATP was measured as described in ref. 13. The rate of ATP synthesis was expressed as a ratio of citrate synthase activity (17).

Oxygen consumption measurements. Respiratory rates of digitonin-permeabilized cells grown in glucose medium were measured at 30°C using a Clark type oxygen electrode as previously described (18). Oxygen consumption measurements were done adding either 10 mmol/L glutamate-10 mmol/L malate plus 0.4 mmol/L ADP (complex I–driven respiration) or 20 mmol/L succinate plus 0.4 mmol/L ADP (complex II–driven respiration) to the protein sample. Respiratory rates (nmol O_2/min/mg protein) were reported after normalization of the polarographic oxygen consumption rates to citrate synthase activity (17).

Respiratory chain oxidoreductase activities. The mitochondrial fraction was isolated from semiconfluent cultures of 150-mm dishes grown in glucose medium as described elsewhere (17). All activities were measured with a dual-wavelength spectrophotometer (V550 extended model, Jasco Europe, Cremella-LC, Italy) at 30°C as described in ref. 19, except mitochondrial protein content for NADH-decyl-ubiquinone reductase (100 μg/mL; ref. 17). Ubiquinol-cytochrome *c* reductase activity, succinate-cytochrome *c* oxidoreductase, and cytochrome *c* oxidase were assayed in the same NADH oxidase buffer conditions (17, 19).

Determination of ROS. XTC.UC1 and TPC-1 cells were seeded and grown in glucose medium for 24 hours in 96-well plates (2×10^4 per well). ROS production was measured after loading with 5 μmol/L dichlorodihydrofluorescein diacetate for 30 minutes (20). After washing, cells were incubated for 1 hour in glucose medium in the presence or absence of 1 μmol/L rotenone, 10 μmol/L antimycin A, or 200 nmol/L carbonyl cyanide *p*-(trifluoro-methoxy)phenylhydrazone. Fluorescence measurements (excitation and emission wavelengths of 490 and 535 nm, respectively) were carried out with a fluorimetric plate reader (Multilabel Counter Victor 2 Wallac 1420). Fluorescence values are normalized for protein content (21) and citrate synthase activity (17).

Western blotting. Cells were collected and resuspended in Laemmli buffer. Protein content was assessed by Coomassie staining (16). For ND1 detection, mitochondrial fractions were lysed as described elsewhere (22). Thirty micrograms of protein were separated by SDS-PAGE electrophoresis and transferred onto nitrocellulose membrane (Amersham Bioscience, Chalfont St. Giles-Bucks, United Kingdom). Mouse antibodies for complex I, II, and IV subunits were used according to the instructions of the manufacturer. Rabbit polyclonal antibodies against the human ND1 subunit and against complex III were used at 1:1,000 dilution. Mouse monoclonal antibody for porin was used at 1:5,000 dilution. Incubation with secondary antibodies and subsequent detection by chemiluminescence were done with the Western Breeze kit according to the instructions of the manufacturer (Invitrogen).

MtDNA sequencing. Total genomic DNA was extracted from cultured cell lines using the phenol/chloroform method according to standard protocols. Genomic DNA (1 ng) was used for amplification with the MitoALL Resequencing kit and PCR amplification was done in a final volume of 10 μL in a 9700 thermal cycler following the conditions given by the manufacturer (Applera, Foster City, CA). PCR products were purified by digestion with 10 units of EXOSAPit (U.S. Biochemical, Cleveland, Ohio) at 37°C for 30 minutes, followed by heat inactivation at 80°C for 15 minutes. The PCR product (5-10 ng) was used for direct sequencing with BigDye kit version 3.1 (Applera). Sequences were run in the ABI 3730 Genetic Analyzer automated sequencing machine.

Electropherograms were analyzed with Sequencing Analysis version 2.5.1 software and inspected with SeqScape version 2.5 software (Applera).

Heteroplasmy evaluation for XTC.UC1 and HXTC cybrid variants. PCR products amplified for ND1 and cytochrome *b* from XTC.UC1 and HXTC cybrid genomic DNA, as described above, were inserted into pcDNA2.1 vector using the TA cloning kit according to the instructions of the manufacturer (Invitrogen). Competent *E. coli* INV5α cells were transformed with the plasmids and selected on Luria-Bertani medium/ampicillin/5-bromo-4-chloro-3-indolyl-β-D-galactopyranoside. White colonies were picked and grown at 37°C in Luria-Bertani medium/100 μg/mL ampicillin. DNA was extracted according to ref. 23 and plasmids were sequenced as described above.

Statistical analysis. All analyses and experiments were repeated at least thrice. The results are presented as the mean ± SD. Statistical analysis was done using the Student's *t* test.

Results

Cell viability and oxidative phosphorylation efficiency. To assess the presence of oxidative phosphorylation defects, growth in galactose medium was determined in the following cell lines:

XTC.UC1, derived from a metastasis of an oncocytic thyroid follicular carcinoma (12); TPC-1, derived from human papillary thyroid carcinoma (24); WRO, derived from human follicular thyroid carcinoma (25); and TAD-2, derived from human fetal thyroid cells (26). As illustrated in Fig. 1*A*, the number of viable TPC-1 cells increased already after 16 hours of incubation in galactose whereas TAD-2, WRO, and XTC.UC1 cells remained unchanged. After 48 to 72 hours of incubation, the number of viable TAD-2 and WRO cells decreased only slightly whereas the XTC.UC1 cells exhibited a significant loss of viability [<15 ± 6% (n = 5), viable after 72 hours].

TPC-1 and XTC.UC1 cells were then chosen for further analysis because they exhibited the most divergent behavior in galactose medium. ATP levels were measured in cells grown either in glucose or in galactose medium. In glucose medium, TPC-1 and XTC.UC1 cell lines had a similar ATP content [6.61 ± 1 (n = 8) and 6.22 ± 0.4 nmol/mg protein (n = 8), respectively]. By replacing glucose with galactose, ATP levels decreased slightly after 8 hours in both cell lines. However, after longer incubation periods, cellular ATP increased to almost the initial value in TPC-1 cells whereas it further decreased in XTC.UC1 cells (Fig. 1*B*). It is therefore apparent that XTC.UC1 cells are unable to survive when forced to rely on the mitochondrial respiratory chain to synthesize ATP.

Further investigation of respiratory chain function was undertaken to identify the defective complex(es) responsible for the energetic failure of XTC.UC1 cells. The rate of ATP synthesis driven by complex I substrates (glutamate plus malate) was found to be dramatically reduced in digitonin-permeabilized XTC.UC1 in comparison with TPC-1 cells, whereas in the presence of the complex II substrate succinate, the reduction was not significantly different (Fig. 1*C*).

The rate of state 3 respiration (i.e., respiration in the presence of phospho-acceptor ADP), determined in digitonin-permeabilized TPC-1 and XTC.UC1 cells, supported by glutamate plus malate, was about half of that obtained using succinate (Fig. 1*D*). Noticeably, in XTC.UC1 cells, the state 3 rate supported by glutamate plus malate was about thrice lower than in TPC-1 cells and the succinate-supported rate was also significantly reduced.

Respiratory complex activities and ROS production. Assessment of mitochondrial respiratory redox activity was done in isolated mitochondria. Complex I activity was assayed using both decyl-ubiquinone and coenzyme Q1 as acceptors (19). The results with these two acceptors were totally overlapping in both cell lines. Sensitivity to the specific inhibitor rotenone (5 μmol/L) was high in both types of cells, indicating that complex I had indeed been assayed rather than contaminating dehydrogenase activities (27, 28). NADH-decyl-ubiquinone oxidoreductase activity in XTC.UC1 mitochondria was found to be very unstable, unlike the activity in mitochondria from TPC-1 cells: after one freeze-thaw cycle, the activity was dramatically decreased (−40%) and became completely rotenone-insensitive (data not shown). Complex I–specific activity, normalized to citrate synthase activity, was found to be significantly lower in XTC.UC1 cells (Fig. 2*A*). Succinate oxidation was measured as cytochrome *c* reductase activity and no significant difference was observed between the oncocytic and control cell lines (Fig. 2*A*; ref. 29).

Complex III activity was assayed using reduced decyl-ubiquinone as the electron donor because this quinone analogue has been shown to be the best substrate in all systems tested (29). The rates of cytochrome *c* reduction were highly sensitive to the specific inhibitor antimycin A. This activity was significantly lower in

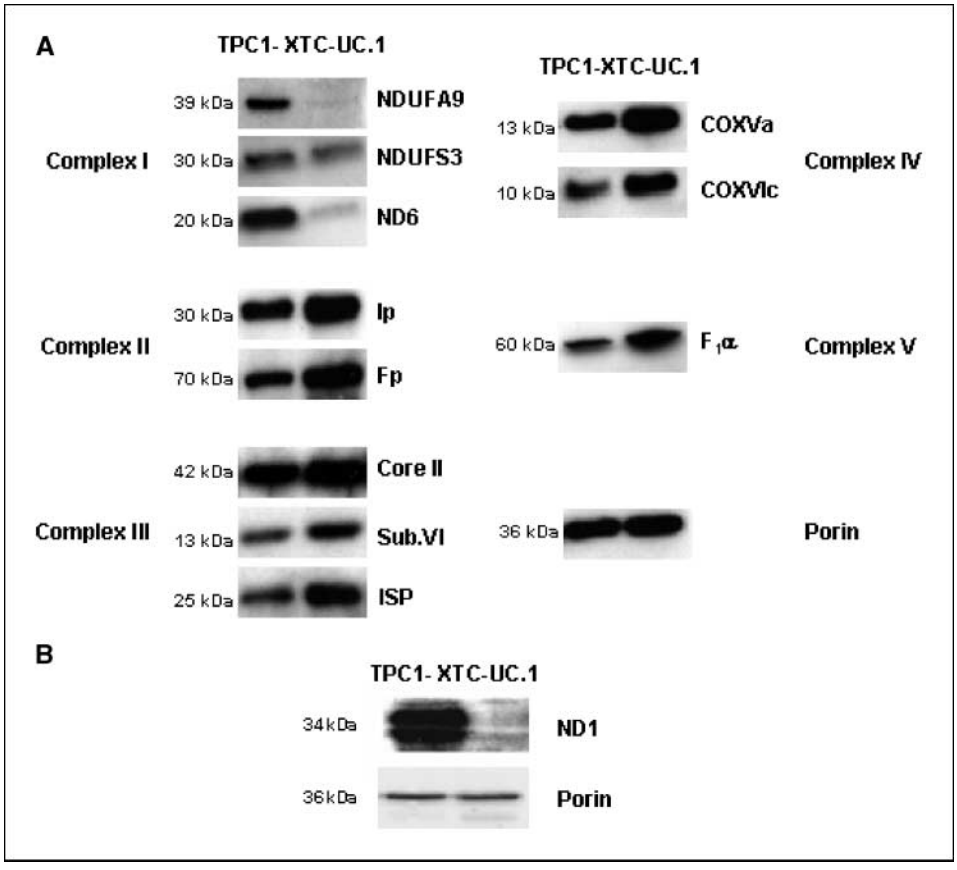

Figure 3. Western blot analysis of mitochondrial proteins. *A,* Western blot analysis of representative subunits of the respiratory complexes and of mitochondrial porin (as a control for loading) was carried out in cell lysates from XTC.UC1 and TPC-1 cells. *B,* Western blot for the ND1 subunit and porin was determined in mitochondrial fractions isolated from XTC.UC1 and TPC-1 cells. Representative of three similar blots.

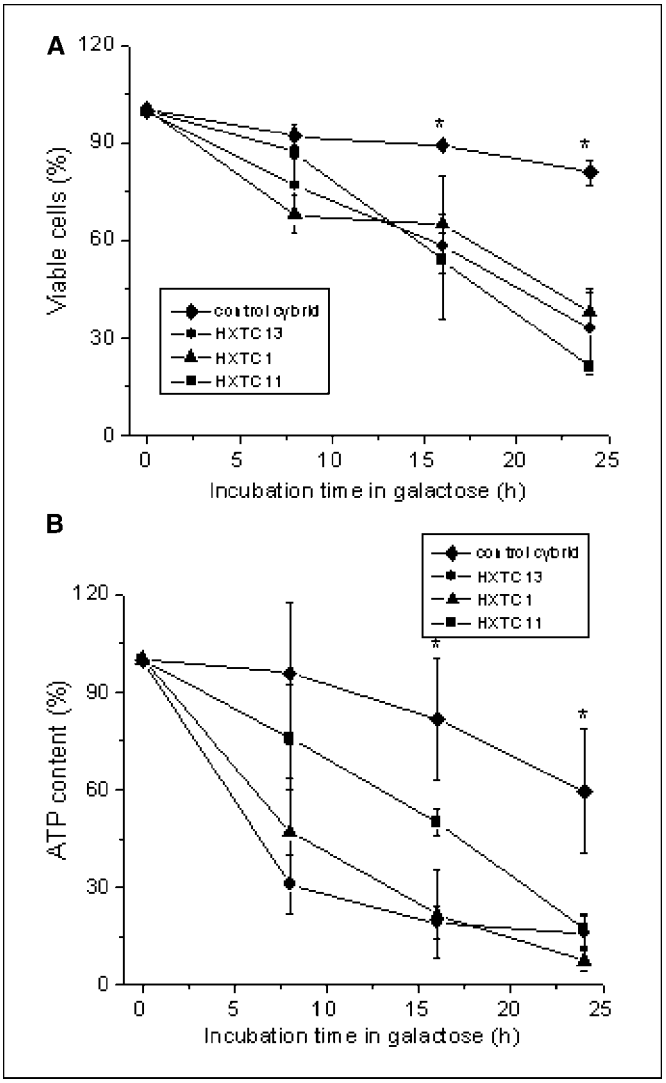

Figure 4. Determination of cell viability and ATP levels in control and HXTC cybrid clones during incubation in galactose medium. Control and HXTC cybrid clones were incubated in DMEM-galactose medium for the times indicated. *A,* cell viability was determined as described in Fig. 1*A*. *Points,* mean of three to five experiments; *bars,* SD. *, $P < 0.01$, values significantly different from that of HXTC cybrid clones. *B,* ATP content was determined as reported in Fig. 1*B*. *Points,* mean of three to four experiments; *bars,* SD. *, $P < 0.05$, values significantly different from that of HXTC cybrid clones.

the oncocytic cells. Cytochrome *c* oxidase was found to be highly active and completely cyanide sensitive, and no significant difference was observed between the two cell lines.

Analysis of the production of ROS showed that, under basal conditions, XTC.UC1 cells produced a significantly higher amount of ROS in comparison with TPC-1 (Fig. 2*B*). ROS generation was not increased by rotenone in either cell line whereas it was strongly stimulated by antimycin A. Interestingly, antimycin A stimulation was lower in the XTC.UC1 cell line. Addition of the uncoupler carbonyl cyanide *p*-(trifluoro-methoxy)phenylhydrazone decreased ROS production only slightly in both cell lines, indicating that reverse electron transfer through complex I is not the main source of oxygen radicals, as suggested for several mitochondrial systems (6).

Analysis of mitochondrial proteins. Western blot analysis for the complex subunits, for which antibodies were available, was done on the two cell lines. The amount of the ND6 and NDUFA9 subunits of complex I was significantly reduced in XTC.UC1 cells whereas several subunits of complex II (Ip and Fp), complex III (core II, subunits VI and ISP), complex IV (COXVa and COXVIc), and complex V (α subunit of ATP synthase) were more abundant in XTC.UC1 when normalized against porin expression (Fig. 3*A*). However, the most striking result was obtained for the ND1 subunit of complex I. Because this protein was detectable only in mitochondrial extracts, Western blot analysis using an antibody specific for human ND1 subunit was done on mitochondrial fractions isolated from XTC.UC1 and TPC-1 cells. As reported in Fig. 3*B*, no band corresponding to the ND1 subunit was detected in mitochondria isolated from XTC.UC1 cells. These results clearly indicate that only the amount of complex I subunits is severely decreased in the oncocytic cell line.

Viability and ATP levels in osteosarcoma-derived cybrids carrying XTC.UC1 mtDNA. To discriminate whether the energetic failure of the XTC.UC1 cell line is due to mtDNA or nuclear DNA mutations, we decided to use the cybrid cell model (30). Cybrids are obtained by fusing a rho-0 cell line (host) completely devoid of mtDNA, with cytoplasts produced by enucleation of cells (donor) containing the mtDNA variants of interest. In this way, the mtDNA of a donor cell can be studied in the context of a "neutral" nuclear background.

We introduced the XTC.UC1 mtDNA into the osteosarcoma 143B.TK$^-$-derived rho-0 cells, obtaining several transmitochondrial cell hybrid (HXTC cybrid) clones. Absence of XTC.UC1 nuclear DNA was tested by using nine different microsatellite markers. The cybrid clones presented a marker profile identical to the parental 143B.TK$^-$ whereas the original XTC.UC1 profile was different (data not shown).

Cell viability and ATP levels of control and of the three HXTC cybrid clones incubated in galactose medium were then determined. Figure 4*A* shows that the viability of all HXTC cybrid clones was significantly decreased in comparison with control cybrids. Accordingly, in controls, ATP levels only slightly decreased after 24 hours, whereas in HXTC clones they were dramatically reduced already after 8 hours of incubation in galactose medium, being significantly different after 16 hours (Fig. 4*B*). After 24 hours, ATP levels in HXTC clones were even lower than in XTC.UC1 parental cells (see Fig. 1*B*). It is worth noting that the reduction of ATP content in control cybrids, but not in HXTC clones, was transient, being the initial value recovered after 48 to 72 hours (data not shown). These results clearly show that HXTC cybrid clones are remarkably more susceptible than control cybrids to the metabolic stress caused by the forced use of oxidative phosphorylation. This observation strongly suggests that the defective respiratory phenotype in HXTC cybrids was transferred with the mitochondrial genome, which most likely carried pathogenic mutations.

Mitochondrial genome sequencing. We sequenced the entire mtDNA of all cell lines tested with the MitoALL kit (Applera). Forty-six overlapping fragments covering the entire 16.5-kb mtDNA were amplified from genomic DNA, directly sequenced on both strands and analyzed with SeqScape version 2.5. As a reference sequence, we used the revised version of the Cambridge Reference Sequence.[7] A list of all the variants identified is reported in Table 1. Several DNA alterations were identified in TPC-1, WRO, and TAD-2 cell

[7] http://www.mitomap.org.

Table 1. Changes identified in thyroid cell lines

(A) Coding changes

Gene	TAD-2		WRO		XTC.UC1		TPC-1	
	Position	Type of amino acid change	Position	Type of amino acid change	Position	Type of amino acid change	Position	Type of amino acid change
ND1	3594C>T[a]	Silent	—		**ins(C) bp3571**	Frameshift G101X	—	—
	4104A>G[a]	Silent	—	—	—	—	—	—
	3693G>A[b]	Silent	—	—	—	—	—	—
	3666G>A[b]	Silent	—	—	—	—	—	—
ND2	4769A>G[a]	Silent	4769A>G[a]	Silent	4769A>G[a]	Silent	4769A>G[a]	Silent
	5393C>T[b]	Silent	—	—	—	—	—	—
	5036A>G[b]	Silent	—	—	—	—	—	—
	5046G>A[a]	V193I	—	—	—	—	—	—
ND3	10398A>G[a]	T114A	—	—	—	—	10398A>G[a]	T114A
ND4	10810T>C	Silent	—	—	—	—	11719G>A[a]	Silent
	10873C>T[a]	Silent	—	—	—	—	11935T>G	Silent
	—	—	—	—	—	—	11939C>A	L394M
	11719G>A[a]	Silent	—	—	—	—	11146C>T	Silent
	—	—	—	—	—	—	11936C>G	L393V
ND4L	10688G>A[b]	Silent	—	—	—	—	—	—
ND5	12519T>C	Silent	14133A>G[a]	Silent	—	—	12361A>G[a]	T9A
	12705C>T[a]	Silent	—	—	—	—	—	—
	13650C>T[a]	Silent	—	—	—	—	—	—
	13789T>C[a]	Y485H	—	—	—	—	—	—
	13880C>A[b]	S515Y	—	—	—	—	—	—
	13105A>G[a]	I257V	—	—	—	—	—	—
	13506C>T	Silent	—	—	—	—	—	—
ND6	14178T>C[a]	I166V	—	—	—	—	1447T>C[a]	Silent
	14560G>A	Silent	—	—	—	—	—	—
	14203A>G[b]	Silent	—	—	—	—	—	—
COX1	6548C>T[b]	Silent	—	—	—	—	—	—
	6827C>T[b]	Silent	—	—	—	—	7028C>T[a]	Silent
	6989A>G[b]	Silent	—	—	—	—	—	—
	7028C>T[a]	Silent	—	—	—	—	—	—
	7055A>G[a]	Silent	—	—	—	—	—	—
	7389T>C[b]	Y496H	—	—	—	—	—	—
	7146A>G[b]	Silent	—	—	—	—	—	—
	7256C>T[a]	Silent	—	—	—	—	—	—
COX2	7867C>T[a]	Silent	—	—	—	—	—	—
	8248A>G	Silent	—	—	—	—	—	—
COX3	9540T>C[a]	Silent	9621G>A	A139T	—	—	9950T>C[a]	Silent
CYTB	14766T>C[a]	I7T	—	—	—	—	15662A>G[a]	I306V
	14769A>G[a]	N8S	—	—	**15557G>A**	**E271K**	15851A>G[a]	I369V
	—	—	—	—	15326A>G[a]	T194A	15326A>G[a]	T194A
	—	—	—	—	—	—	14766C>T	T7I
	15115T>C[a]	Silent	—	—	—	—	C15223C>T	Silent
	15326A>G[a]	T194A	15326A>G[a]	T194A	—	—	15508C>T	Silent
ATP6	8655C>T[a]	Silent	8618T>C[a]	I131T	—	—	8584G>A[a]	A20T
	8701A>G[a]	T59A	—	—	8860A>G[a]	T112A	8860A>G[a]	T112A
	8860A>G[a]	T112A	8860A>G[a]	T112A	—	—	8829C>T[a]	Silent
ATP8	8468C>T[a]	Silent	—	—	—	—	—	—

(Continued on the following page)

lines; however, most of them are silent polymorphisms or do not produce any coding changes and have been previously reported.[7] This also suggests that cellular differences in growth rate in galactose medium were not due to mtDNA variants and they could all be considered as controls for XTC.UC1 cell viability. The potential effect of each missense substitution (either novel or already reported) on protein structure and function was evaluated *in silico* using PolyPhen program (Polymorphism Phenotyping), which predicts the potential effect of amino acid substitutions on protein structure and activity (31). All the missense variants identified in TPC-1, WRO, and TAD-2 cells were benign (data not shown).

Table 1. Changes identified in thyroid cell lines (Cont'd)

(B) Noncoding changes

Gene	TAD-2	WRO	XTC.UC1	TPC-1
	Position	Position	Position	Position
TRNT	—	—	—	15927G>A
RNR1	709G>A[a]	—	—	ins(C) bp960[c]
	710T>C[a]	—	—	—
	750A>G[a]	750A>G[a]	—	709G>A
	769G>A[a]	—	750A>G[a]	750A>G[a]
	825T>A[a]	—	1438A>G[a]	1438A>G[a]
	1018G>A	—	—	1598G>A
RNR2	2352T>C[a]	3010G>A[a]	3010G>A[a]	2706A>G[a]
	1738T>C[c]	—	—	—
	2768A>G	—	—	—
	2885T>C[a]	—	—	—
	2706A>G[a]	—	—	—
	2758G>A[a]	—	—	—
TRNH	—	—	—	12192G>A
TRND	7521G>A[a]	—	—	—
TRNA	5655T>C[a]	—	—	—
Displacement loop	16126T>C[a]	16172T>C[a]	16189T>C[a]	16140C>T[a]
	16170A>T	16192C>T[a]	16356T>C[a]	16138A>T[a]
	16187C>T[a]	16456G>A[a]	16362T>C[a]	16189T>C[a]
	16189T>C[a]	16519T>C[a]	16519T>C[a]	16223C>T[a]
	16223C>T[a]	207G>A[a]	263A>G[a]	16243T>C[a]
	16264C>T[a]	263A>G[a]	ins(C) bp315[a]	16318A>T[a]
	16270C>T[c]	—	del(AC) bp523[c]	16319G>A
	16278C>T[a]	—	—	16519T>C
	16311T>C[a]	—	—	del(AC) bp523[c]
	16390G>A[a]	—	—	—
	16519T>C[a]	—	—	—
	73A>G[a]	—	—	—
	152T<C[a]	—	—	—
	182C>T[a]	—	—	—
	185G>T[a]	—	—	—
	195T>C[a]	—	—	—
	247G>A[a]	—	—	—
	263A>G[a]	—	—	—
	357A>G[a]	—	—	—
	del(AC) bp523[c]	—	—	—

NOTE: All variants were compared with the public databases (http://www.mitomap.org) and are classified as follows: (*a*) polymorphisms already published; (*b*) unpublished polymorphisms; and (*c*) changes associated with disorders other than thyroid carcinomas: 1738T>C (reported in the case of colon cancer), 16270C>T (reported in the case of oral cancer), del(AC) bp523 (reported in PEO), and ins(C) bp960 (reported in case of deafness). In (A) the coding variants are reported. The deleterious mutations in XTC.UC1 are shown in bold. In (B) changes identified in tRNAs, rRNA, and the displacement loop are reported.

Interestingly, a C insertion at bp3571 was identified in XTC.UC1 (Fig. 5*A*). This frameshift mutation inserts a premature stop codon at amino acid 101 in the ND1 subunit of complex I, thus generating a truncated ND1 protein, which could explain the data from Western blot analysis showing a complete absence of the full-length ND1. No lower band could be detected for the truncated form (data not shown); thus, it might be hypothesized that the short pathologic variant is degraded early on. A second mutation, 15557G>A, was identified in XTC.UC1, which inserts a nonconservative missense substitution, E271K, in cytochrome *b*, the only mtDNA-encoded subunit of complex III (Fig. 5*B*). For both changes, heteroplasmy was evaluated by insertion of the relative PCR products into the pcDNA2.1 vector, transformation in the *E. coli* strain INV5α, and analysis of ~50 clones for each mutation. The mutation in ND1 was found to be heteroplasmic, with a 5.7% presence of the wild-type allele (6C stretch) and a 94.3% presence of the mutated allele (7C stretch), whereas for the mutation in cytochrome *b*, heteroplasmy was evaluated as 29.7% of the wild-type allele (G) and 70.3% of the mutated allele (A).

The two changes in ND1 and in cytochrome *b* were absent in a large collection of ~2,000 healthy individuals[8] and the ND1

[8] A. Achilli and A. Torroni, personal communication.

mutation was also reported as an "unpublished" mutation in a case of parathyroid neoplasia in the mitochondrial variant database.[7]

The mutation in cytochrome *b* corresponding to the E271K substitution affects an amino acid, which is completely conserved throughout evolution. PolyPhen analysis was also done for this mutation and it showed that it is probably damaging (position-specific independent count score, 1.753).

All HXTC cybrid cell clones were also tested for the presence of the two specific XTC.UC1 mitochondrial mutations and heteroplasmy was measured as previously described. All the clones were found to carry the mutations in ND1 and cytochrome *b*; however, some differences in the degree of heteroplasmy were observed. For the ND1 mutation, the presence of the wild-type allele (6C) was between 5% and 7.4% in all clones. Conversely, for cytochrome *b* mutation, we detected percentages of the wild-type allele of 42%, 50%, and 73% in HXTC1, HXTC13, and HXTC11 clones, respectively. The higher percentage of heteroplasmy determined in HXTC11 in comparison with other clones is likely to be responsible for the slow decrease of ATP content during incubation in galactose medium (Fig. 4*B*), suggesting that the oxidation of substrates through complex II/III may partially compensate for the complex I impairment.

Discussion

In the present study, we show for the first time that the occurrence of a severe energetic dysfunction in a thyroid oncocytic cell model can be attributed to two pathogenic mtDNA mutations: the first is a frameshift mutation in the gene encoding ND1 subunit of complex I, which generates a truncated version of the ND1 protein; the second mutation is a missense substitution in the cytochrome *b* gene, which affects the catalytic site involved in the electron transfer of complex III. Both mutations were found to be heteroplasmic and were predicted to have a pathogenic role, the first resulting in the absence of the ND1 subunit and the second affecting an invariant amino acid position.

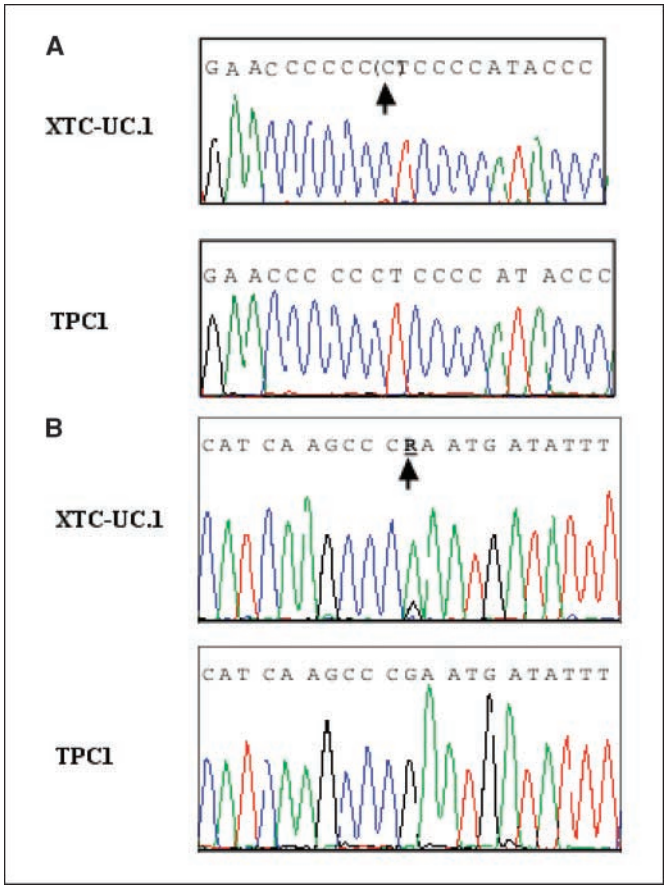

Figure 5. Sequence analysis of mtDNA variants in XTC.UC1. Electropherograms showing the C insertion in ND1 gene (*A*) and the missense variant in cytochrome *b* (*B*) identified in XTC.UC1 cells versus TPC-1 sequence.

Detailed biochemical analysis showed that XTC.UC1 cells are unable to grow after forced use of oxidative phosphorylation. Furthermore, in XTC.UC1 cells, the rates of mitochondrial ATP synthesis and oxygen consumption driven by complex I substrates were dramatically decreased in comparison with TPC-1 cells. Conversely, in the presence of complex II substrate, the difference between the two cell lines was less relevant. Accordingly, NADH-decyl-ubiquinone oxidoreductase activity was also significantly lower in the oncocytic cells and, in addition, was very unstable, unlike the activity in control mitochondria. A low respiratory rate has also been reported in mitochondrial disorders caused by maternally inherited mtDNA defects, such as Leber's hereditary optic neuropathy, wherein mutations in the ND4, ND1, and ND6 subunits of complex I hamper the physiologic electron transfer to oxygen through the respiratory chain (18, 32–34).

In XTC.UC1 cells, Western blot analysis showed an up-regulation of some subunits of the respiratory complexes, most likely due to a compensatory effect for the energetic impairment. The ND1 protein was completely absent; although at the DNA level a small amount of the wild-type allele was present, the amount of wild-type protein produced may be insufficient to be detected. However, the fact that expression of the ND6 subunit was also remarkably reduced in the oncocytic cells suggests possible derangements in complex I assembly through the generation of subsequent subcomplexes (35). In particular, subcomplex formation may be impaired by the absence of ND1 in XTC.UC1, as shown in Leigh's syndrome, wherein mutations in ND6 cause a defective complex I assembly (36). The presence of an ND1-truncating mutation in XTC.UC1 provides a further model with which to study the detailed steps of complex I assembly.

The other novel mutation identified in XTC.UC1 cells is a heteroplasmic mutation that affects the cytochrome *b* gene. In agreement with this finding, a significant decrease in complex III activity was identified in the oncocytic cell line. Although this amino acid substitution is predicted to be deleterious, it is possible that the percentage of the wild-type cytochrome *b* allele is sufficient to complement the pathogenic effects at the cellular level, and this would hence explain why the activity of complex III, although reduced, still remains higher than both the rates of NADH and succinate oxidation. Further studies are needed to address the exact role of this mutation in relation to the oncocytic phenotype and to establish a heteroplasmy threshold for expressing the pathogenic effect of this mutation on complex III activity.

The dramatic increase in ROS production in the oncocytic cell line is compatible with the decrease in activity of both complexes I and III, the major mitochondrial sources of ROS (7). The relative quantitative relevance of mitochondrial and extramitochondrial sources of ROS production (27) cannot be evaluated under the experimental conditions used. Nevertheless, it is of interest that the stimulation by antimycin A is less prominent in XTC.UC1 cells, perhaps indicating that basal ROS production is higher per se in their mitochondria. Significantly, the results are in accordance with the enhanced ROS generation observed in inherited complex I deficiencies (37–41).

Although several reports to date have identified mtDNA variants in different types of tumors, thus far, no clear direct link has been established about their pathogenic role. A causative role of nuclear-encoded mitochondrial proteins has previously been shown for specific tumors (42). Recent reports show a frequent recurrence of mtDNA variants in complex I, III, IV, and V subunit genes in thyroid oncocytic tumors (8, 43) although no direct link was made between any specific bioenergetic defect and these mtDNA variants. A useful experimental approach to investigate the cellular phenotype associated with mtDNA mutations is provided by the cybrid cellular model. The results reported here strongly show that the energetic failure in the XTC.UC1-derived cybrid clones is due to mtDNA mutations present in the XTC.UC1 parental cells, ruling out a role for nuclear DNA. The next most interesting step will be to detect the prevalence of such mutations in stabilized cell lines of oncocytic thyroid tumors, as well as in primary tumors. Preliminary data from our group suggest that disruptive mutations are also found in the mtDNA of pathologic specimens derived from thyroid oncocytic tumors.[9] Defects in the mitochondrial respiratory chain leading to decreased energy production primarily affect tissues with high energy requirements and render cells unable to adapt to conditions of reduced mitochondrial energy supply. This might explain how mtDNA mutations in the thyroid, an organ with elevated energy consumption, might promote aberrant cellular growth leading to the oncocytic phenotype. Interestingly, complex I defects induce mitochondrial outgrowth as a consequence of increased ROS production (44). It is therefore tempting to speculate that the oncocytic character of these tumors is due to stimulation of mitochondrial proliferation by ROS.

In conclusion, mtDNA mutations identified in the oncocytic XTC.UC1 cells and the related mitochondrial energy dysfunction could represent biomarkers for oncocytic tumors and may contribute to the development of specific treatments for this potentially lethal form of thyroid cancer.

[9] Unpublished results.

Acknowledgments

Received 1/16/2006; revised 4/5/2006; accepted 4/7/2006.

Grant support: Associazione Italiana per la Ricerca sul Cancro grant 1145 (G. Tallini), Fondo per gli investimenti della ricerca di base (Rome), and the European Commission Project QLRT-2000-01646 (G. Romeo).

The costs of publication of this article were defrayed in part by the payment of page charges. This article must therefore be hereby marked *advertisement* in accordance with 18 U.S.C. Section 1734 solely to indicate this fact.

We thank Dr. Raimo Tanzi and Dr. Federico Sebastiani (Applera) for technical assistance and helpful suggestions, and Dr. Martha Hoque for correction of the manuscript.

References

1. Tallini G. Oncocytic tumours. Virchows Arch 1998;433:5–12.
2. Sobrinho-Simoes M. Follicular carcinoma in World Health Organization classification of tumors—pathology and genetics. In: DeLellis RA, Lloyd RV, Heitz PU, Eng C, editors. Tumors of endocrine organs. Lyon: IARC Press; 2004. p. 72.
3. Maximo V, Sobrinho-Simoes M. Hurthle cell tumours of the thyroid. A review with emphasis on mitochondrial abnormalities with clinical relevance. Virchows Arch 2000;437:107–15.
4. Rustin P. Mitochondria, from cell death to proliferation. Nat Genet 2002;30:352–3.
5. Wallace DC. A mitochondrial paradigm of metabolic and degenerative diseases, aging, and cancer: a dawn for evolutionary medicine. Annu Rev Genet 2005;39:359–407.
6. Lenaz G. The mitochondrial production of reactive oxygen species: mechanisms and implications in human pathology. IUBMB Life 2001;52:159–64.
7. Maximo V, Sobrinho-Simoes M. Mitochondrial DNA 'common' deletion in Hurthle cell lesions of the thyroid. J Pathol 2000;192:561–2.
8. Rogounovitch T, Saenko V, Yamashita S. Mitochondrial DNA and human thyroid diseases. Endocr J 2004;51:265–77.
9. Savagner F, Chevrollier A, Loiseau D, et al. Mitochondrial activity in XTC UC1 cells derived from thyroid oncocytoma. Thyroid 2001;11:327–33.
10. Savagner F, Franc B, Guyetant S, Rodien P, Reynier P, Malthiery Y. Defective mitochondrial ATP synthesis in oxyphilic thyroid tumors. J Clin Endocrinol Metab 2001;86:4920–5.
11. Robinson BH, Petrova-Benedict R, Buncic JR, Wallace DC. Nonviability of cells with oxidative defects in galactose medium: a screening test for affected patient fibroblasts. Biochem Med Metab Biol 1992;48:122–6.
12. Zielke A, Tezelman S, Jossart GH, et al. Establishment of a highly differentiated thyroid cancer cell line of Hurthle cell origin. Thyroid 1998;8:475–83.
13. Zanna C, Ghelli A, Porcelli AM, Martinuzzi A, Carelli V, Rugolo M. Caspase-independent death of Leber's hereditary optic neuropathy cybrids is driven by energetic failure and mediated by AIF and endonuclease G. Apoptosis 2005;10:997–1007.
14. Ghelli A, Zanna C, Porcelli AM, et al. Leber's hereditary optic neuropathy (LHON) pathogenic mutations induce mitochondrial-dependent apoptotic death in transmitochondrial cells incubated with galactose medium. J Biol Chem 2003;278:4145–50.
15. Manfredi G, Yang L, Gajewski CD, Mattiazzi M. Measurements of ATP in mammalian cells. Methods 2002;26:317–26.
16. Bradford MM. A rapid and sensitive method for the quantitation of microgram quantities of protein utilizing the principle of protein-dye binding. Anal Biochem 1976;72:248–54.
17. Trounce IA, Yoon LK, Jun AS, Wallace DC. Assessment of mitochondrial oxidative phosphorylation in patient muscle biopsies, lymphoblasts, and transmitochondrial cell lines. Methods and Enzymol 1996;264:484–509.
18. Baracca A, Solaini G, Sgarbi G, et al. Severe impairment of complex I-driven adenosine triphosphate synthesis in Leber hereditary optic neuropathy cybrids. Arch Neurol 2005;62:730–6.
19. Genova ML, Castelluccio C, Fato R, et al. Major changes in complex I activity in mitochondria from aged rats may not be detected by direct assay of NADH:coenzyme Q reductase. Biochem J 1995;311:105–9.
20. McLennan HR, Degli Esposti M. The contribution of mitochondrial respiratory complexes to the production of reactive oxygen species. J Bioenerg Biomembr 2000;32:153–62.
21. Lowry OH, Rosebrough NJ, Farr AL, Randall RJ. Protein measurement with the folin phenol reagent. J Biol Chem 1951;193:265–75.
22. Porcelli AM, Ghelli A, Zanna C, Valente P, Ferroni S, Rugolo M. Apoptosis induced by staurosporine in ECV304 cells requires cell shrinkage and up-regulation of Cl− conductance. Cell Death Differ 2004;11:655–62.
23. Sambrook J, Fritsch EF, Maniatis T. Molecular cloning: a laboratory manual. Cold Spring Harbor (NY): Cold Spring Harbor Laboratory Press; 1991.
24. Ishizaka Y, Ushijima T, Sugimura T, Nagao M. cDNA cloning and characterization of ret activated in a human papillary thyroid carcinoma cell line. Biochem Biophys Res Commun 1990;168:402–8.
25. Pang XP, Hershman JM, Chung M, Pekary AE. Characterization of tumor necrosis factor-α receptors in human and rat thyroid cells and regulation of the receptors by thyrotropin. Endocrinology 1989;125:1783–8.
26. Martin A, Huber GK, Davies TF. Induction of human thyroid cell ICAM-1 (CD54) antigen expression and ICAM-1-mediated lymphocyte binding. Endocrinology 1990;127:651–7.
27. Lenaz G, Fato R, Genova ML, Formiggini G, Parenti-Castelli G, Bovina C. Underevaluation of complex I activity by the direct assay of NADH-coenzyme Q reductase in rat liver mitochondria. FEBS Lett 1995;366:119–21.
28. Genova ML, Bovina C, Marchetti M, et al. Decrease of rotenone inhibition is a sensitive parameter of complex I damage in brain non-synaptic mitochondria of aged rats. FEBS Lett 1997;410:467–9.
29. Degli Esposti M, Rotilio G, Lenaz G. Effects of dibromothymoquinone on the structure and function of the mitochondrial bc1 complex. Biochim Biophys Acta 1984;767:10–20.
30. King MP, Attardi G. Human cells lacking mtDNA: repopulation with exogenous mitochondria by complementation. Science 1989;246:500–3.
31. Ramensky V, Bork P, Sunyaev S. Human non-synonymous SNPs: server and survey. Nucleic Acids Res 2002;30:3894–900.
32. Majander A, Huoponen K, Savountas ML, Nikoskelainen E, Wikstrom M. Electron transfer properties of NADH:ubiquinone reductase in the ND1/3460 and the ND4/11778 mutations of the Leber hereditary neuroretinopathy (LHON). FEBS Lett 1991;292:289–92.
33. Carelli V, Ghelli A, Bucchi L, et al. Biochemical features of mtDNA 14484 (ND^/M64V) point mutation associated with Leber's hereditary optic neuropathy. Ann Neurol 1999;45:320–8.
34. Brown MD, Trounce IA, Jun AS, Allen JC, Wallace DC. Functional analysis of lymphoblast and cybrid mitochondria containing the 3460,11778, or 14484 Leber's hereditary optic neuropathy mitochondrial DNA mutation. J Biol Chem 2000;275:39831–6.
35. Vogel R, Nijtmans L, Ugalde C, van den Heuvel L, Smeitink J. Complex I assembly: a puzzling problem. Curr Opin Neurol 2004;17:179–86.
36. Ugalde C, Triepels RH, Coenen MJ, et al. Impaired

complex I assembly in a Leigh syndrome patient with a novel missense mutation in the ND6 gene. Ann Neurol 2003;54:665–9.
37. Pitkanen S, Robinson BH. Mitochondrial complex I deficiency leads to increased production of superoxide radicals and induction of superoxide dismutase. J Clin Invest 1996;98:345–51.
38. Luo X, Pitkanen S, Kassovska-Bratinova S, Robinson BH, Lehotay DC. Excessive formation of hydroxyl radicals and ladehydic lipid peroxidation products in cultured skin fibroblast from patients with complex I deficiency. J Clin Invest 1997;99: 2877–82.
39. Vergani L, Martinuzzi A, Carelli V, et al. MtDNA mutations associated with Leber's hereditary optic neuropathy: studies on cytoplasmic hybrid (cybrid) cells. Biochem Biophys Res Commun 1995;210:880–8.
40. Floreani M, Napoli E, Martinuzzi A, et al. Antioxidant defences in cybrids harboring mtDNA mutations associated with Leber's hereditary optic neuropathy. FEBS J 2005;272:1124–35.
41. Miranda S, Foncea R, Guerrero J, Leighton F. Oxidative stress and up-regulation of mitochondrial biogenesis genes in mitochondrial DNA-depleted HeLa cells. Biochem Biophys Res Commun 1999; 258:44–9.
42. Eng C, Kiuru M, Fernandez MJ, Aaltonen LA. A role for mitochondrial enzymes in inherited neoplasia and beyond. Nat Rev Cancer 2003;3:193–202.
43. Maximo V, Soares P, Lima J, Cameselle-Teijeiro J, Sobrinho-Simoes M. Mitochondrial DNA somatic mutations (point mutations and large deletions) and mitochondrial DNA variants in human thyroid pathology: a study with emphasis on Hurthle cell tumors. Am J Pathol 2002;160:1857–65.
44. Koopman WJH, Visch HJ, Verkaart S, van der Heuvel WJP, Smeitink JA, Willems PHGM. Mitochondrial network complexity and pathological decrease in complex I activity are tightly correlated in isolated human complex I deficiency. Am J Physiol Cell Physiol 2005;289:C881–90.